

BIOCHE 1831

# Closed state of gramicidin channel detected by X-ray in-plane scattering

K. He, S.J. Ludtke, Y. Wu, H.W. Huang \*

*Physics Department, Rice University, Houston, TX 77251 (USA)*

O.S. Andersen

*Department of Physiology and Biophysics, Cornell Univ. Med. College, New York, NY 10021 (USA)*

D. Greathouse and R.E. Koeppe II

*Department of Chemistry and Biochemistry, University of Arkansas, Fayetteville, AR 72701 (USA)*

(Received 20 June 1993; accepted in final form 4 October 1993)

## Abstract

An analogue of gramicidin A (gA) was synthesized with the formyl group replaced by a BOC group. The analogue (BOC-gA) exhibited single channel conduction, but the channel is 5-order-of-magnitude destabilized relative to the gA channel. Hydrated mixtures of gramicidin and dilauroyl phosphatidylcholine in the molar ratio of 1:10 were prepared into uniformly aligned multiple bilayers, and X-ray scattering with the momentum transfer in the plane of the membrane was measured. Analysis with the help of computer simulations showed that 70% of BOC-gA are monomers. Thus for the first time it was shown that gramicidin monomers are stable inside the monolayers of a lipid membrane. Furthermore, the monomers have the same  $\beta$  helical conformation as the dimeric channel. The result suggests the possibility that when a gramicidin channel is closed, it dissociates into two monomers floating in opposite monolayers.

**Keywords:** Gramicidin; X-ray scattering; Monomers; Lipid membranes

## 1. Introduction

Recently we have demonstrated a technique of X-ray scattering with its momentum transfer ori-

ented in the plane of a membrane [1,2]. As an application, we showed that the scattering curve of gramicidin in membrane is consistent with the dimeric channels being randomly distributed in the plane of the membrane. This result resolved the question of whether the gramicidin channel forms aggregates in its conducting form. As a further application of X-ray in-plane scattering,

\* Corresponding author.

we now investigate the conformation of the closed state of gramicidin.

Gramicidin, a linear pentadecapeptide, forms the best understood ion channels in bilayer membranes. A vast body of experimental evidence indicates that the gramicidin channel is a cylindrical pore consisting of two monomers, each a single-stranded  $\beta^{6.3}$  helix, hydrogen-bonded head-to-head at their *N* termini [3–5]. The pore selectively facilitates the diffusion of monovalent cations across bilayer membranes, but do not transmit anions or divalent cations [5,6]. The single-channel properties of the channel are well characterized. In particular, the closing of the channel appears to be a simple first-order process [5,6]. Because of such (relative) simplicity, gramicidin has been used extensively as a testing ground for theory and experiment of ion conduction through a protein pore [5].

One major remaining unknown concerning the mechanism of the gramicidin channel is what is its closed state; that is, what happens to the channel when it stops conducting. At least three possibilities have been suggested: (a) The head-to-head dimer becomes an intertwined dimer, the crystal form of gramicidin grown from organic solvents [7]. (b) The dimer dissociates into two monomers in opposing monolayers and each remains in the  $\beta$  helical form. Or (c) The monomers exit the bilayer onto the membrane surface and assume an unspecified form, because the monomers are unstable in the bilayers [6]. Although circular dichroism (CD) is sensitive to secondary structures, it cannot discriminate between a dimeric form and a monomeric form of gramicidin in the  $\beta$  helical conformation. Here we will show that the technique of in-plane scattering can make a distinction among these three cases. Natural gramicidin tends to be in the dimeric channel form at concentrations high enough for X-ray detection. To create the non-conducting state of gramicidin, we synthesized an analogue in which the formyl group of the natural gramicidin A (gA) is replaced by a BOC group – we will call this BOC-gramicidin (BOC-gA). In the single-channel experiments, BOC-gA exhibited 1000-fold reduced channel forming potency and 200-fold shorter mean channel duration, to-

gether a 5-order-of-magnitude destabilization of the dimeric channel compared with gA. (The method of preparation of BOC-gA and its single-channel experiment will be published elsewhere.)

## 2. X-ray in-plane scattering

The technique of X-ray in-plane scattering was described in ref. [1]. The principle for analyzing the in-plane scattering curve was also given. The idea of the present experiment is very simple. We will prepare two similar samples, one with BOC-gA and another with nature gramicidin, which for our purpose is equivalent to gA. In the previous papers [1,2] we have shown that the scattering curve of gA represents freely diffusing gramicidin dimers in the bilayers. If the BOC-gA are also dimers, either in the  $\beta$  helical form or the intertwined form (the case a), the scattering curve would be indistinguishable from that of gA. (The lengths and radii of a  $\beta$  helical dimer and an intertwined dimer are about the same [7,8]; therefore they have practically the same electron density projected onto the plane of the membrane.) If the BOC-gA are monomers and remain embedded in the monolayers (the case b), its scattering curve would be exactly one-half of that of gA. (This is because in this case two monolayers are independent; each monolayer with gramicidin monomers is equivalent to a bilayer with dimers, except that the form factor of a monomer is one-half of that of a dimer; and the scattering intensity is proportional to the square of the form factor and to the number of independent layers.) However, if the BOC-gA are partly dimers and partly monomers, the scattering curve would be between 50% and 100% of the gA curve. Finally, if the case c were true, the scattering curve would be characteristically different from that of gA.

Hydrated mixtures of gramicidin, dilauryl phosphatidylcholine, and thallium acetate (in the molar ratio of 1:10:1) were prepared into uniformly aligned multiple bilayers [8,9] between two SiO<sub>2</sub>-coated, polished beryllium plates. Thallium ions have a large binding constant to the gramicidin channel [8]; they are used to enhance the

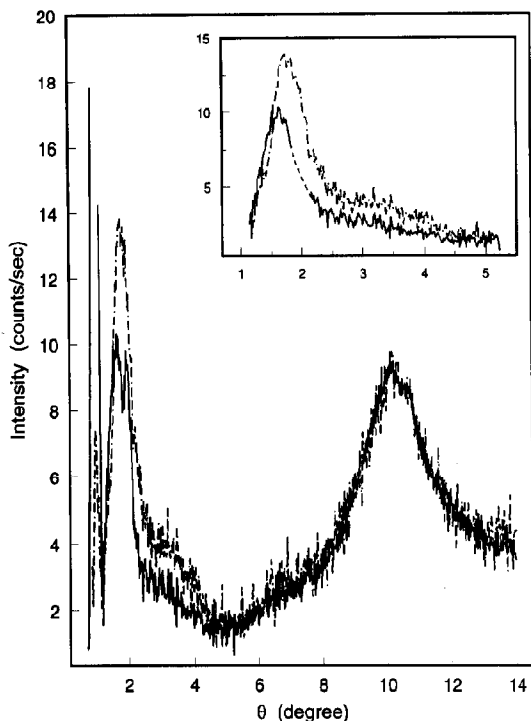


Fig. 1. In-plane scattering intensity of DLPC bilayers containing gramicidin with thallium ions in the molar ratio 10:1:1 (gA dashed line, BOC-gA solid line). The bands near  $10^\circ$  are due to the lipid chains; they are used to normalize the two scattering curves. The sharp peaks near  $1^\circ$  and  $2^\circ$  are the lamellar diffraction peaks of the first and second order, due to the presence of smectic defects in the multilayer samples (see ref. [1] for details). The features between  $1^\circ$  and  $5^\circ$  are the scattering curves due to the gramicidins; they are isolated in the inset with the lamellar peaks removed (dashes).

X-ray contrast (the relative electron density) of gramicidin against the lipid background. In such a preparation, gA is known to be in the dimeric channel form [8]. On the other hand, we had no prior knowledge about the condition of BOC-gA. Circular dichroism indicated that BOC-gA was in the  $\beta$  helical configuration (the same as gA [8,9]), but whether it was in the dimeric or monomeric form was unknown. (It is possible that thallium ions tend to induce BOC-gA into the  $\beta$  helical conformation.) In-plane scattering was performed by  $\theta$ - $2\theta$  scan [1,2]. Fig. 1 shows the scattering curves of gA and BOC-gA in DLPC bilayers at the same peptide/lipid molar ratio  $P/L = 1/10$ . The two curves were put on the same scale by

matching the lipid peaks at  $\theta \approx 10^\circ$  [1]. The curve of BOC-gA is similar to that of gA, but its amplitude is smaller by about 30% and the whole curve is shifted to smaller angles, specifically, the main peak is shifted from  $1.74^\circ$  to  $1.63^\circ$ . Thus the result is not as simple as we expected, but we will see that a definitive conclusion can be reached nevertheless. Firstly, the scenario (c) is excluded as a possible explanation because lamellar diffraction shows that the thallium ions are well inside the bilayer, indicating that the peptides are embedded in the bilayers (see below). Now we have to understand what can cause a shift in the peak position.

In the previous papers [1,2] we have shown that a scattering curve can be converted into a radial distribution curve, which expresses the distribution of the molecules relative to an arbitrarily chosen one. The first major peak of the radial distribution function gives the average distance to the nearest neighbors,  $d_{nn}$ . Numerically  $d_{nn}$  is approximately (within 10% error) equal to  $7.0/q_{max}$  (1), where  $q_{max}$  is the position of the first (main) peak of the scattering curve expressed as a function of the momentum transfer  $q = 4\pi \sin\theta/\lambda$ . Thus a smaller  $q_{max}$ , as in the case of BOC-gA (fig. 1) implies a larger  $d_{nn}$ . Together with a smaller amplitude, the BOC-gA scattering curve appears, at first sight, to be explainable as due to a lower concentration. Thus we checked the concentrations of our samples in two ways. First, each experimental curve was reproduced by at least two different batches of samples independently prepared at different times. Second, after the X-ray experiment, the peptide to lipid molar ratio  $P/L$  of the sample was measured. The peptide concentrations were determined by UV absorption and the lipid concentrations were determined by a modified Fiske-SubbaRow method [9]. The  $P/L$  of the gA and BOC-gA samples were found to be 1.0/9.5 and 1.0/9.8, respectively.

### 3. Computer simulation

Various theoretical techniques for computing X-ray scattering intensity have been described by

Hansen and McDonald [10]. In particular, if the scattering particles are hard spheres, the Percus–Yevick approximation produces analytical solutions for the scattering curve in three dimensions, that can be compared directly with experimental data. Unfortunately the Percus–Yevick equation has not been successfully solved in two dimensions. And other analytical techniques are also troublesome in this dimensionality. Thus, we resort to the methods of molecular dynamics and Monte Carlo [10]. We consider a bilayer. Each monolayer contains  $N$  harddisks of radius  $R$ . The harddisks are either monomers or dimers; a dimer is formed by two monomers from opposite monolayers. The monomers of the same monolayer interact by a hardcore repulsion. The monomers of different monolayers do not interact with each other, whereas a dimer interacts with the other dimers as well as with the monomers of both monolayers. In the Monte Carlo method, the harddisks diffuse randomly in the two-dimensional plane with the constraint that interacting harddisks can not overlap with each other. In the molecular dynamics simulation, the harddisks are given initial random velocities and followed by elastic collisions [1]. After the system reaches equilibrium, the scattering intensity  $I_s = |\sum_j s_j \exp(i\mathbf{q} \cdot \mathbf{r}_j)|^2$  was calculated, where  $\mathbf{q}$  is the momentum transfer of the X-ray scattering,  $\mathbf{r}_j$  is the position of the  $j$ th harddisk in the plane, and  $s_j$  is one or two if the  $j$ th harddisk is a monomer or a dimer, respectively. The form factor of the harddisk is otherwise not included in  $I_s$ . We found the results from the two methods consistent with each other, as expected; therefore, we will present only the Monte Carlo results.

First we investigated the effect of concentration. Fig. 2 shows the simulated scattering intensities of dimeric disks in three different concentrations. The radius  $R$  was chosen to be 9 Å; this is the estimated radius of the gramicidin channel [1]. The numbers of the disks  $N$  were chosen so that the areal densities of the harddisks are equivalent to that of the gramicidin in a bilayer at  $P/L$  equal to 1/10, 1/20, and 1/30, respectively. (The cross section of the DLPC molecule is about 52 Å<sup>2</sup>.) To compare the simulated curves with the

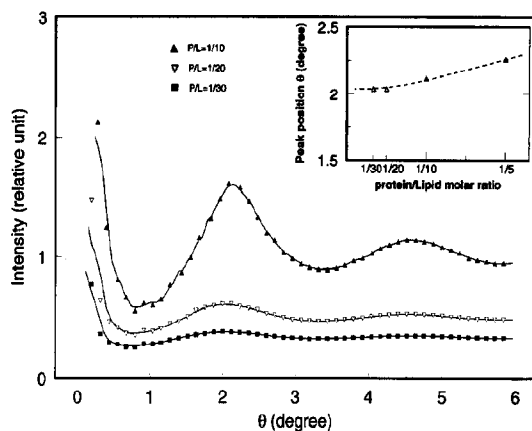


Fig. 2. The simulated scattering intensities of harddisks of radius 9 Å at three different concentrations equivalent to  $P/L = 1/10$ ,  $1/20$ , and  $1/30$ . The position of the first peak is shown as a function of  $P/L$  in the inset.

experimental data, the latter should be divided by the square of a ( $q$ -dependent) form factor of the gramicidin channel [1,2]. However the form factor is a slowly varying function of  $q$  [1,2]; the division by the form factor squared does not affect the peak position of the scattering curve within the experimental errors. Therefore, for the problem under consideration, the form factor may be ignored. We see from the simulations that the peak position is rather insensitive to the concentration. For example to produce a 6% shift in the peak position (from  $1.74^\circ$  to  $1.63^\circ$ ), the concentration has to change from  $L/P = 1/10$  to  $L/P = 1/20$ . Thus we concluded that the difference in the peak position between the two samples observed in fig. 1 is not due to a concentration difference.

On the other hand, the peak position is very sensitive to the disk radius. Fig. 3 shows three simulation curves with the disk radius  $R = 7$ , 9, and 11 Å, respectively. The number of the disks  $N$  was chosen so that at  $R = 9$  Å the areal density of the disks is equivalent to  $P/L = 1/10$ . The peak position  $\theta_{\max}$  of the simulated intensity is related to the radius  $R$  by the empirical relation  $2Rq_{\max} = 5.5$ . It is clear from these simulation results that the peak position of a scattering curve is largely determined by the radius  $R$  and is relatively insensitive to the density. Thus the scattering curve of gA in fig. 1, which has  $\theta_{\max} = 1.74^\circ$

or equivalently  $q_{\max} = 0.248 \text{ \AA}^{-1}$ , can be reproduced by harddisks of  $R = 12 \text{ \AA}$  and  $P/L = 1/10$  (2). The scattering curve of BOC-gA which has the peak position  $\theta_{\max} 1.63^\circ$  corresponds to harddisks of  $R = 12.7 \text{ \AA}$ .

It should be stressed that in interpreting the scattering curve in terms of harddisks, the radius  $R$  does not necessarily represent the molecular size of the gramicidin channel. The correct interpretation is that  $R$  represents the effective radius of the channel–channel interaction. In other words,  $2R$  represents the closest distance two channels approaching each other. Since the radius of the gramicidin channel is about  $9 \text{ \AA}$  and the size of a lipid molecule is about  $5 \text{ \AA}$  by  $10 \text{ \AA}$ , the result  $R \sim 12 \text{ \AA}$  seems to indicate that there is always at least one lipid molecule between two channels. We do not have an explanation of why the effective interaction radius of BOC-gA is slightly larger than that of gA.

How do we explain the difference in the amplitude between the BOC-gA and the gA scattering curves? From figs. 2 and 3, it is clear that, excluding the possibility of dimer–monomer conversion, the peak amplitude and peak width are mainly determined by the areal density occupied by the disks – the higher the areal density, the larger the amplitude and the narrower the width. If the BOC-gA and the gA are both dimers, the

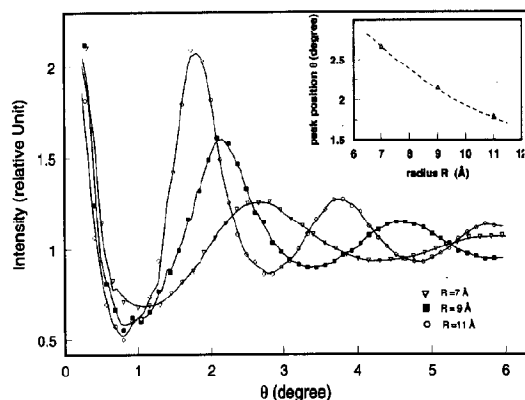


Fig. 3. The simulated scattering intensities of harddisks of three different radii,  $R = 7, 9,$  and  $11 \text{ \AA}$ . The number of the disks  $N$  was chosen so that at  $R = 9 \text{ \AA}$  the areal density of the disks is equivalent to  $P/L = 1/10$ . The position of the first peak is shown as a function of  $R$  in the inset.

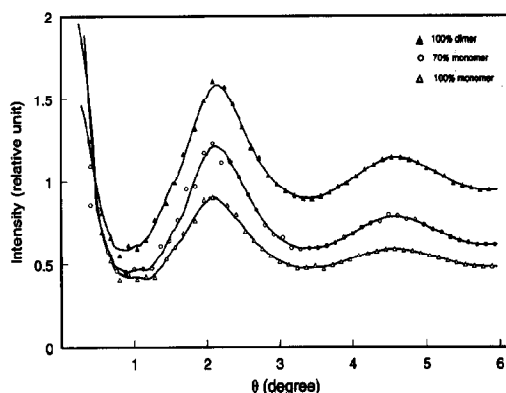


Fig. 4. The simulated scattering intensities of 100% dimers, a combination of 30% dimers and 70% monomers and 100% monomers.  $R = 9 \text{ \AA}$ ,  $P/L = 1/10$ .

larger effective radius should give the BOC-gA a larger amplitude, like the example shown in fig. 3. Therefore a smaller amplitude at a smaller  $\theta_{\max}$  for BOC-gA is incompatible with the BOC-gA being all dimers. The simplest explanation for a reduced amplitude is that a substantial fraction of the BOC-gA is in the monomeric form. fig. 4 shows the simulated intensities of pure dimers, pure monomers, and mixtures. A 30% reduction in amplitude from that of pure dimers indicates that about 70% of the disks are monomers.

#### 4. Lamellar diffraction

The technique of lamellar diffraction (with the momentum transfer perpendicular to the plane of the membrane) and the procedure for its data analysis have been described previously [8,11]. We performed lamellar diffraction on the same samples used in the in-plane scattering. In addition, samples containing gramicidin without thallium and samples of pure DLPC were also measured. Fig. 5 shows the diffraction patterns of the gA and BOC-gA samples as well as a sample of pure DLPC containing no gramicidin. The phases of the diffraction amplitudes were determined by the swelling method. Conversion to the electron density profiles,  $\rho$ , is shown in fig. 6. From the difference density profile,  $\rho(\text{with thallium}) - \rho(\text{without thallium})$ , we obtain the distribution of

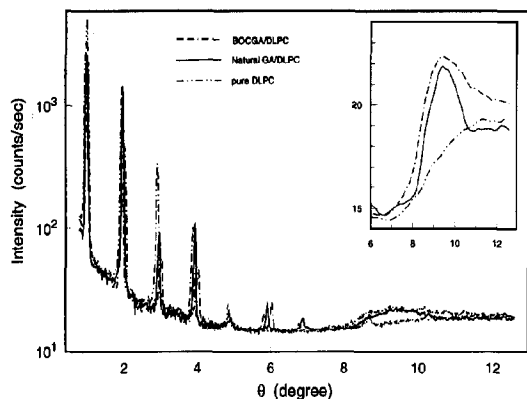


Fig. 5. Lamellar diffraction of three different samples: BOC-gA in DLPC bilayers, gA in DLPC bilayers, and DLPC bilayers without gramicidin; the same samples produced Fig. 1. The intensities between  $6^\circ$  and  $12^\circ$  are magnified in the inset. Unlike in-plane scattering (fig. 1), there is no reference band for normalizing these diffraction patterns.

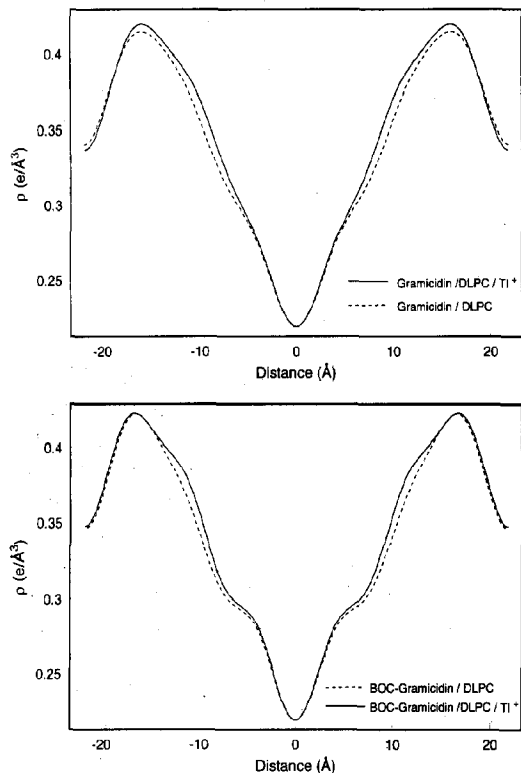


Fig. 6. The electron density profiles of gA in DLPC bilayer with and without thallium ions (top), and BOC-gA in DLPC bilayer with and without thallium ions (bottom).

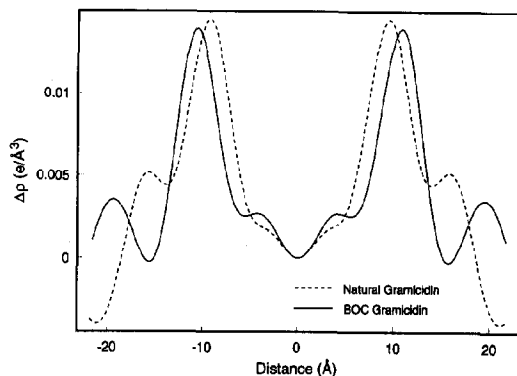


Fig. 7. The difference electron density profiles obtained from fig. 6 show the distributions of thallium ions in the bilayer, with gA (dotted line) and with BOC-gA (solid line).

thallium ions across the bilayer (fig. 7). We see that the peaks representing the binding sites are well within the bilayer, indicating that in both cases, gA and BOC-gA, gramicidin binds the ions and the peptide is embedded in the hydrophobic region of the bilayer. The ion-binding sites of gA have been discussed previously in ref. [8]. Further discussion on the binding sites of BOC-gA will be published elsewhere.

The band due to the helical structure of gramicidin [12] was also recorded around  $9.5^\circ$  in fig. 5. It is clear that the bands are due to the presence of gramicidin. The peak position  $\theta = 9.45^\circ \pm 0.05^\circ$  corresponds to a repeating structure of  $4.69 \pm 0.02 \text{ \AA}$ , somewhat different from the predicted pitch,  $4.97 \text{ \AA}$ , of a  $\beta^{6.3}$  helix [13]. ( $4.97 \text{ \AA}$  is equivalent to  $8.86^\circ$ .) What is important here is that the bandwidth of BOC-gA is clearly larger than the bandwidth of gA. Since the band width is inversely proportional to the number of repeating units, the helix of BOC-gA is on average shorter than that of gA. This result is consistent with the in-plane scattering; i.e. a substantial fraction of BOC-GA are in the monomeric form.

## 5. Conclusion

We have observed the gramicidin monomers residing inside the monolayers of a lipid mem-

brane. The monomers have the same  $\beta$  helical conformation like the dimeric channel. This result suggests the possibility that when a channel is closed, it dissociates into two monomers floating in opposite monolayers.

### Acknowledgement

This research was supported in part by the Department of Energy grant DE-FG03-93ER-61565, the Robert A. Welch Foundation, the Office of Naval Research grant N00014-90-J-1020, and the National Institutes of Health Biophysics Training Grant GM08280.

### References

- 1 K. He, S.J. Ludtke, Y. Wu and H.W. Huang, *Biophys. J.* 64 (1993) 157.
- 2 K. He, S.J. Ludtke, Y. Wu and H.W. Huang, *J. Phys.* IV Paris, to be published.
- 3 D.W. Urry, in: *The enzymes of biological membranes*. Vol. 1, ed. A.N. Martonosi (Plenum Press, New York, 1985) p. 229.
- 4 A.S. Arseniev, A.L. Lomize, I.L. Barsukov and V.F. Bystrov, *Biol. Membranes* 3 (1986) 1077.
- 5 O.S. Andersen and R.E. Koeppe, *Physiol. Rev.* 72S (1992) 89.
- 6 S.B. Hladky and D.A. Haydon, in: *Current topics in membranes and transport*. Vol. 21, ed. F. Bronner (Academic Press, New York, 1984) p. 327.
- 7 F.R. Salemme, *Science* 241 (1988) 145; B.A. Wallace and K. Ravikumar, *Science* 241 (1988) 182; D.A. Langa, *Science* 241 (1988) 188.
- 8 G.A. Olah, H.W. Huang, W. Liu and Y. Wu, *J. Mol. Biol.* 218 (1991) 847.
- 9 H.W. Huang and G.A. Olah, *Biophys. J.* 51 (1987) 989.
- 10 J.P. Hansen and I.R. McDonald, *Theory of simple liquids* (Academic Press, New York, 1976), pp. 90–140.
- 11 H.W. Huang, W. Liu, G.A. Olah and Y. Wu, *Progr. Surface Sci.* 38 (1991) 145.
- 12 J. Katsaras, R.C. Prosser, R.H. Stinson and J.H. Davis, *Biophys. J.* 61 (1992) 827.
- 13 H. Monoi, *Biophys. J.* 64 (1993) 36.